Penerbit Akademia Baru

Journal of Advanced Research in Fluid Mechanics and Thermal Sciences

Journal homepage: www.akademiabaru.com/arfmts.html
ISSN: 2289-7879

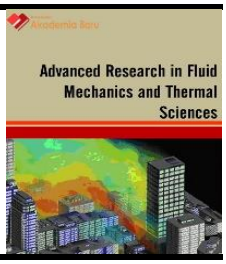

Temperature Dependence of Quantum Dots-in-well Infrared Photodetectors (QDIPs) Using Photoluminescence

Open Access

Noor Hafidzah Jabarullah [1,*]

[1] Universiti Kuala Lumpur Malaysia Institute of Aviation Technology, Jalan Jenderam Hulu, Kampung Jenderam Hulu, 43900 Sepang, Selangor Malaysia

ARTICLE INFO

Article history:
Received 12 November 2019
Received in revised 20 January 2019
Accepted 25 January 2019
Available online 10 February 2019

ABSTRACT

A study of quantum dots-in-well infrared photodetectors (QDIPs) yields results useful for the creation of a two-colour QDIP. Quantum dot infrared photodetectors (QDIPs) have been shown to be a key technology in mid and long wavelength infrared detection due to their potential for normal incidence operation and low dark current. This study investigates infrared detectors based on intersubband transitions in a novel InAs/In0.15 Ga0.85 As/GaAs quantum dots-in-well (DWELL) heterostructure. In the DWELL structure, the InAs quantum dots are placed in an In0.15 Ga0.85 As well, which in turn is placed in GaAs quantum well with In0.1Ga0.9As barrier. The optical properties of the sample have been studied by the means of photoluminescence using fourier transform infrared spectroscopy. Spectrally tuneable response with bias and long wave IR response at 6.2µm and 7.5µm has been observed.

Keywords:
Quantum Dots, Infrared, Photodetectors

1. Introduction

High performance infrared (IR) photodetection is desirable for many applications involving thermal imaging, chemical analysis, night vision, remote sensing, space ranging, mine detection and fibre-optic communications [1]. Depending upon the application, one may desire either different specifications, either a broad, multicolour response from the detector, or a sharp single wavelength response [2]. Multicolour IR detection has the ability to determine the temperature of the observed body, in addition to producing images with some colour depth, so is much more favourable for a general imaging system [3]. Multi-colour focal plane array (FPA) photodetectors are particularly useful for medical and military imaging as well as environmental monitoring applications.

Quantum dots-in-well DWELL are part of a new technology of semiconductor nano-photonic devices, utilising stacked layers of quantum dots (QDs) as the active region in their structures [4]. DWELL photodetectors are a promising new advancement that will hopefully overcome many of the shortcomings of existing IR photodetection systems [5]. QDIPs utilise inter-subband absorption to detect medium and long wavelength infrared radiation within the low absorption, 3-5µm & 8-14µm

* *Corresponding author*
E-mail address: nhafidzah@unikl.edu.my (Noor Hafidzah Jabarullah)

atmospheric 'windows' [6]. There has been significant research into the study of QDIPs, but little in the way of multi-colour QDIP development, despite their desirability for a wide variety of applications [7]. The aim of this project is to obtain the optical properties of the sample by photoluminescence and photocurrent measurement while analysing the advantages and disadvantage of quantum-dots-in-well photodetector. This paper involves on studying the combination or hybrid of quantum-dot and quantum-well, which is known as dot-in-well (DWELL) and optimising the advantages by this hybrid system the theory of the QDIP. The aim of this paper is to study the optical properties of the DWELL QDIP sample using experimental techniques. The experimental work on this project focuses studying the optical properties by the means of photoluminescence

1.1 Energy Band Structure

Figure 1 shows schematic of the DWELL structure and the energy band profile for the sample structure is illustrated in Figure 2 [8]. The valence band offset (VBO) of the $Al_{0.1}Ga_{0.9}As$, GaAs, $In_{0.15}Ga_{0.8}As$ and InAs is -1.33eV, -0.8eV, -0.38eV and -0.59eV respectively.

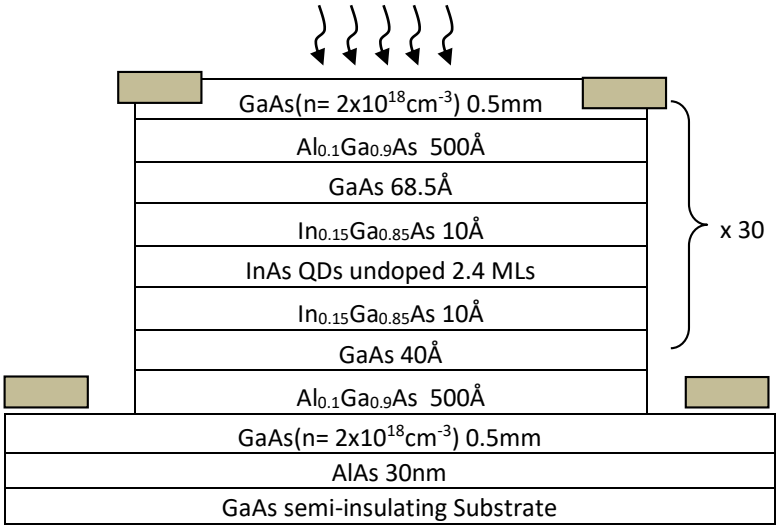

Fig. 1. Heterostructure of schematic of InAs/ $In_{0.15}Ga_{0.8}As$/GaAs dots-in-well infrared photodetector

The room temperature PL spectrum obtained from this InAs/ $In_{0.15}Ga_{0.8}As$/GaAs dots-in-well infrared photodetector QDIP is shown in Figure 3. The PL wavelength of the InAs is 1255nm showing that this device is crucial to achieve quantum efficiency without introducing dislocations.

Infrared photodetectors with an InAs/ $In_{0.15}Ga_{0.8}As$/GaAs DWELL active region suffer from strain related issues. Due to high compressive strain, a greater number of active region layers cannot be grown without introducing dislocations. More layers will enhance the absorption, which in turn increases the quantum efficiency,η of the photodetector [9]. This increase in η will increase the responsivity and detectivity of the detectors [10].In order to determine the energy levels it is necessary to include the effects due to strain on the structure [11]. The energy values of the QW's are affected by the strain the layers [12]. GaAs has a direct energy gap at the Γ point of 1.519 and InAs has a direct energy gap of 0.417 at the Γ point. Thus, the value of $In_{0.15}Ga_{0.8}As$ is less of GaAs and has been obtained from the ternary calculation depending on the alloy composition using a simple quadratic equation.

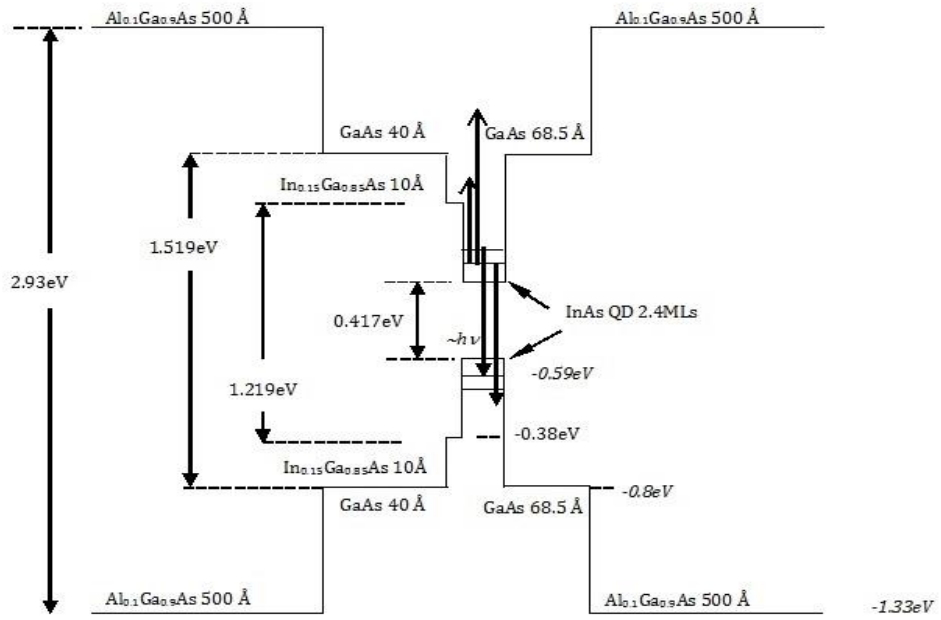

Fig. 2. The unstrained energy band structure

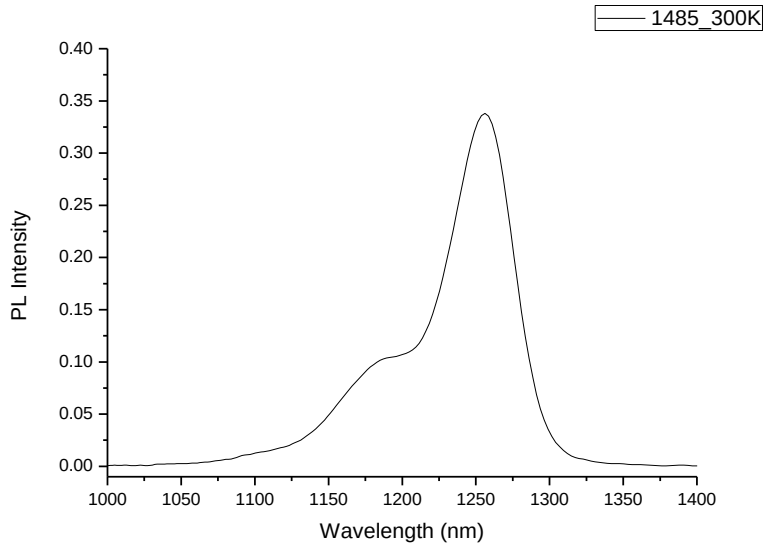

Fig. 3. Room temperature PL for the 30-period this InAs/ $In_{0.15}Ga_{0.8}As$/GaAs

$$E_g(A_{1-x}\,B_x) = (1-x)E_g(A) + xE_g(B) + x(1-x)C \quad (1)$$

where C is the bowing parameters that has been obtained from linear interpolation between the two A and B binaries[13].

The lattice mismatch between the substrate, the QWs and the other material in the sample is not too large, so when the mismatch is less than 7%, it is assumed that no misfits are generated at the interfaces by compression or expansion of the planes [12, 13]. This means that the strain in the materials consist of uniform biaxial strain (hydrostatic) parallel to the interface and unaxial strain parallel to the growth direction. The hydrostatic component of compressive strain increases the bandgap and tensile strain reduces the bandgap. The strain effects not only on the band edges but also modifies the effective massed associated with the individual bands. The strained-induced of the

bulk material responds to the shift of energies in QWs and barrier heights. The hydrostatic strain is obtained using below equation:

$$\varepsilon_{\parallel} = \varepsilon_{xx} = \varepsilon_{yy} = \frac{a_s - a_e}{a_e} \quad (2)$$

$$\varepsilon_{zz} = -2\frac{C_{12}}{C_{11}} \quad (3)$$

where ε_{xx}, ε_{yy} and ε_{zz} are diagonal strain components of strain tensor is defined to be negative for compressive strain. a_s, is the lattice constant for the substrate and a_e, is the epilayer lattice constant. C_{12} and C_{11} is the elastic constants. The material parameters for the calculation of bandgap, VBO and strain are taken from Vurgaftman & Meyer (2001).

Energy bandgap change in the conduction band, ΔE_c and valence band, ΔE_v is given by:

$$\Delta E_c = a_c(\varepsilon_{xx} + \varepsilon_{yy} + \varepsilon_{zz}) \quad (4)$$

$$\Delta E_v = a_v(\varepsilon_{xx} + \varepsilon_{yy} + \varepsilon_{zz}) \quad (5)$$

From the Bir-Pikus strain interaction it is not sufficient to describe the full effect of the valence band strain. Shear deformation potential, *b* is necessary to explain the shear deformation that split the valence band into heavy/light hole. The + and – signs refer to heavy and light hole respectively.

In order to calculate the ΔE_c and ΔE_v for the ternary materials linear interpolation between the binary data obtain from Vurgaftman & Meyer (2001) is used to determine the values if the parameters used. It has been calculated that very small lattice constant difference between the substrate and the epilayer materials, very small strain value to the energy gap produced by the calculation. The QWs calculation was performed using formulas obtained from [14] and [15] by PhD student in the group. The QDs strain can only be obtained using numerical calculation therefore, in this study values are obtained from numerical calculation using finite element method. Figure 4 shows the strained conduction band profile produced numerically.

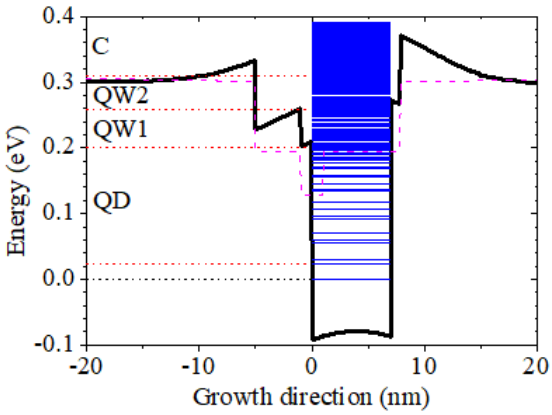

Fig. 4. The strained conduction band for InAs/ $In_{0.15}Ga_{0.8}As$/GaAs DWELL through the centre of the QD (solid line) and through the QW without crossing the dots (dashed line)

2. Methodology

2.1 Device Fabrication

The samples used in this study are grown in a VG Semicon V-80 molecular beam epitaxy in the ESPRC National Centre for III-IV semiconductor Technology [16]. The InAs/In0.15Ga0.8As/GaAs dots-in-well (DWELL) structure is grown on a GaAs semi-insulating substrate with 30 periods of the DWELL. These active regions of 30 layers are separated by 500Å thick of Al0.1Ga0.9As barriers. The DWELL layers consist of 2.4MLs of InAs in a 20Å of In0.15Ga0.8As quantum well (QW) which in turn is surrounded by GaAs QW. Device fabrication is done in a class-100 clean room where the 400µm x 400µm mesas were defined using photolithography, followed by metal evaporation and then etching techniques. The first stage was to define the mesa structure for the QDIPs using standard photolithography (Figure 5) [17].

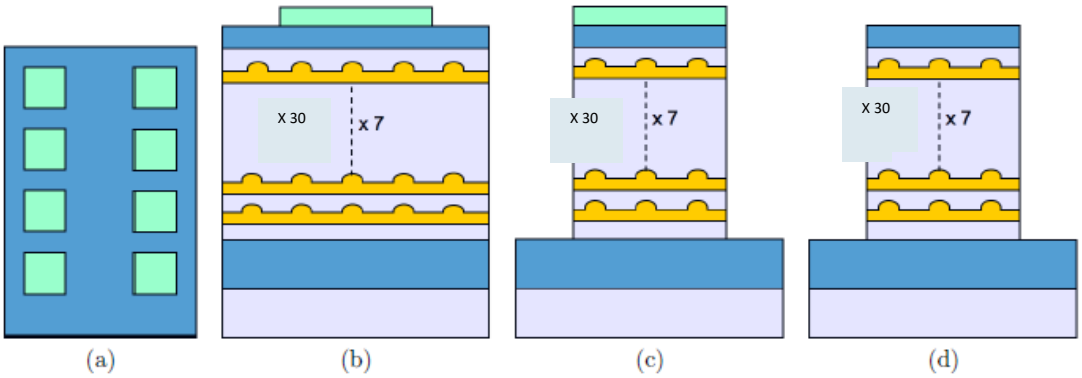

Fig. 5. The schematic of the mesa structure processes. (a) The top view of the patterned sample, with the photoresist marked in light blue. (b) The sample cross-section with the photoresist square on top. (c) Cross-section etching process. (d) A single mesa cross-section after photoresist been removed

The second stage was the formation of the metal contacts and the final packaging [18]. Another photolithography step was carried out to define areas for the metal contacts on the QDIPs. The lithography procedure described in the steps above was repeated using a different mask for the metal contacts. The pattern for the contacts consisted of leaving clear circles of 200µm diameter on top of each mesa and long clear rails on the bottom contact layer, with the rest of the sample covered in photoresist. This will allow each QDIP on the sample would have an independent top contact and a shared bottom contact. After the second photolithography step, metal contacts were formed first removing of natural oxidation by cleaning the sample in HCl (10%) for 40s. The using evaporation method, layers of Ge, Ni and Au been deposited for the n-type metal contacts. After that is the lift off process by using acetone to remove the photoresist from the sample. The final step consists of annealing the contacts using rapid thermal annealing under N_2 flow at 400°C for 45 seconds The device was finally packaged by mounting it on a 12-pin TO5 header, with 25µm thick gold wires were bonded to the metal contacts on all the QDIPs in the sample, connecting them to the gold pins on the header.

2.2 Photoluminescence (PL) Measurement

Photoluminescence (PL) is the spontaneous emission of light from a material's optical excitation used to investigate the optical properties of the samples. PL investigations can be used to

characterize both intrinsic electronic transitions and electronic transitions at impurities as well as defects in semiconductors and insulators. PL is the typical technique used for characterization of III-IV semiconductors due to the advantage of non-destructive, non electrical contact which requires minimal effort for sample preparation PL detects the optical transition from an excited electronic state to lower electronic states, usually the ground states (Figure 6). Only transitions from the lower electronic states can generally be observed at low temperatures because of rapid thermalisation. Most of the light results from the difference in energy of the excited electron returning to its ground state.

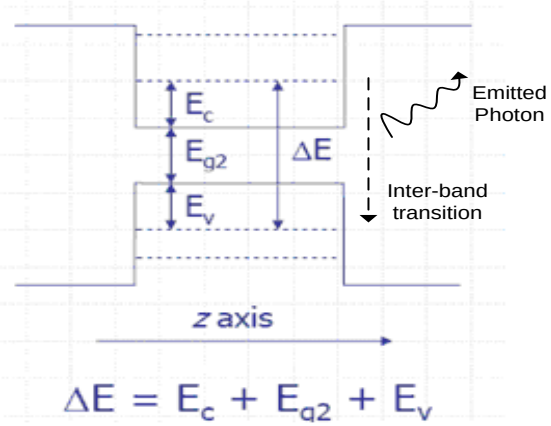

Fig .6. Photoluminescence mechanism and relationship with electronic band structure

The PL spectra have narrow band which makes the analysis possible[19]. The position of PL peaks is related to the energy of each excited level and can be used as sensitive probe to find impurities and other defects in semiconductors. The PL intensity can give more information on the quality of interfaces and surfaces. PL spectrum and the dependencies on its intensity on the irradiation intensity and device temperature provide important information for device characterisation. PL spectra and the intensity can be used determine the energy gap or wavelength of maximum gain, understand the component of ternary/quaternary layers its impurity levels and allows for the understanding and investigations of the recombination mechanism investigations[20] The PL measurement were completed using a Fourier Transform Infrared (FTIR) spectroscopy, FTIR is an efficient and dynamic technique that provides qualitative and quantitative information which require a broadband range from Near-IR to Far-IR spectrum. FTIR spectrometer collects and examines all wavelengths simultaneously instead of viewing each one separately. This technique is known as Felgett or multiplex advantage [21]. The interferometer will produce infrared spectra by collecting the interferogram of a sample that involves Fourier Transform mathematical manipulation that can involve phase correction and apodization.

3. Results and Discussion

3.1 Temperature Dependence

The spectra show a main peak, with a higher energy (ground state) lower intensity (excited state) shoulder. As temperature is reduced, the spectrum shifts towards the red which is to higher wavelengths. As to the variation of peak emission intensity with temperature, it appears that the peak intensity increases slightly as temperature is increased from 78K, peaking at 125K, before reducing substantially towards 300K.

For purposes of clarity, the spectra in Figure 7 were all normalized and plotted in Figure 8. It is clear that the spectral main peak red-shifted with reducing of temperature, where at 78K the ground state peak is at 2.24µm and reducing to 1.9µm at 300K. The higher energy shoulder is visible in each spectrum as well.

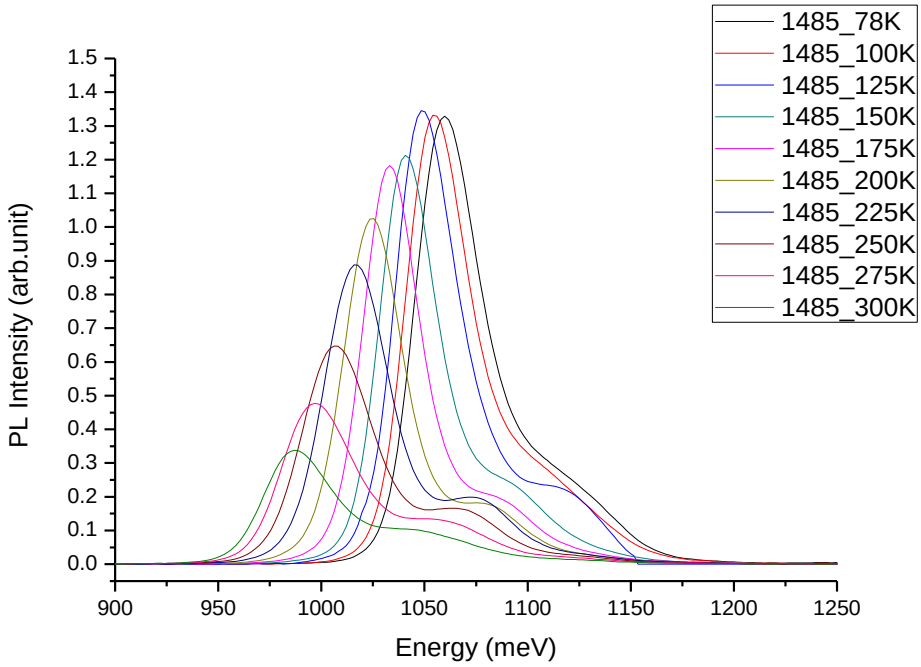

Fig. 7. PL spectra for sample VN1485 at temperatures from 78K to 300K

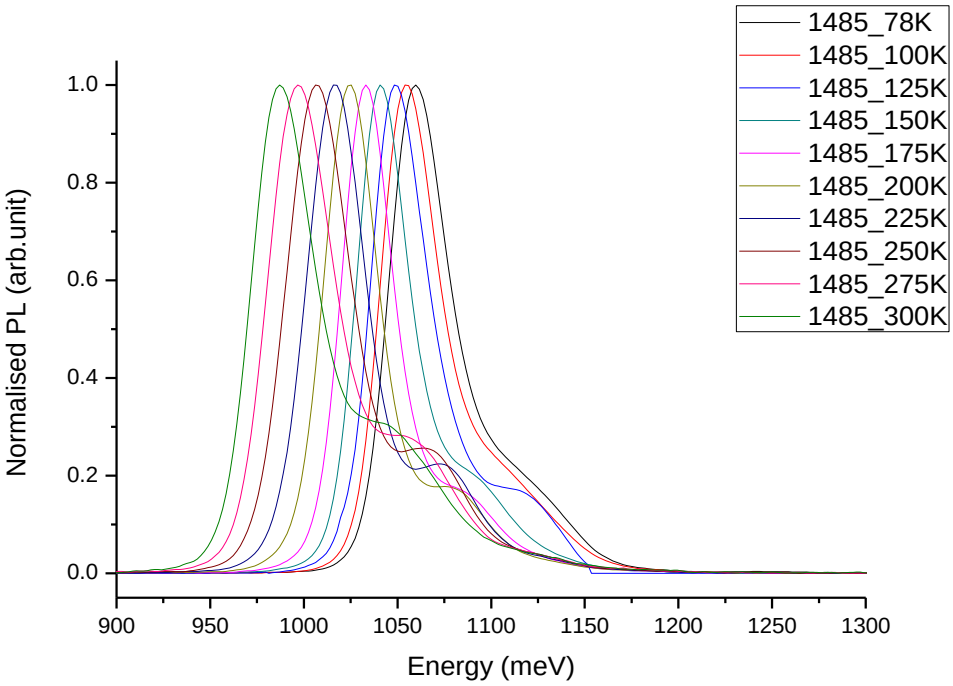

Fig. 8. Normalised PL spectra for sample VN1485 at temperatures from 78K to 300K

To aid in the analysis, the data was fitted to two Gaussian curves (e.g. Figure 8, at 225K), the sum of which would account for a main peak and shoulder. The curve fitting tool in OriginLab was applied to the spectral data, with fits made to using fit linear curve. The integrated intensity was then obtained by numerical integration of the Gaussian curves.

At 78K the PL transition energy is found to be 1.14eV from the experimental result,and comparing to the modelling calculation provided by the optoelectronics research group it is assumed that the Ga content, x in the InAs dot is between 30%. The modelling result is based on undoped material only therefore no comparison can be made for the doped sample.

4. Conclusions

This paper has presented the mid-wavelength infrared QDIP with 30-layers of DWELLs in the active region where special attention has been given to the optical properties of the intersubband photodetector namely the DWELL detector. The photoluminescence and photocurrent of the device has been investigated.

The results have demonstrated impressive outcome which is good control over the operating wavelength, higher operating temperature and bias tunable spectral. The photoresponse of the DWELL showed a dependence on the applied bias due to the tilting of the conduction band edge and the change in probability of tunnelling from the quantum well excited states through the barriers. By changing the bias it is possible to tune the wavelength window of the detector

Acknowledgement

Special acknowledgement to Professor Stephanie Haywood for he endless support in this project. We also would like to acknowledge University of Hull and EPSRC National Epitaxy in University of Sheffield for their facilities to be utilised for this project.

References

[1] Kasap, Safa, and Peter Capper, eds. *Springer handbook of electronic and photonic materials*. Springer, 2017..

[2] Adhikary, Sourav, and Subhananda Chakrabarti. "In (Ga) As/GaAs Quantum Dot Infrared Photodetectors (QDIPs) with Quaternary Capping." In *Quaternary Capped In (Ga) As/GaAs Quantum Dot Infrared Photodetectors*, pp. 33-45. Springer, Singapore, 2018.

[3] Krishna, Sanjay. "Quantum dots-in-a-well infrared photodetectors." *Journal of Physics D: Applied Physics* 38, no. 13 (2005): 2142.

[4] Ghadi, H., S. Dubey, P. K. Singh, M. Bhatt, and S. Chakrabarti. "Highly efficient InAs/InGaAs quantum dot-in-a-well heterostructure validated with theoretically simulated model." In *Quantum Dots and Nanostructures: Growth, Characterization, and Modeling XV*, vol. 10543, p. 105430S. International Society for Optics and Photonics, 2018..

[5] Sengupta, Saumya, and Subhananda Chakrabarti. "Introduction to Infrared Detectors and Quantum Dots." In *Structural, Optical and Spectral Behaviour of InAs-based Quantum Dot Heterostructures*, pp. 1-11. Springer, Singapore, 2018.

[6] Gupta, Rita, A. L. Y. Wong, and S. K. Haywood. "3\mu m Intersubband Quantum Well Photodetector (QWIP)." *Turkish Journal of Physics* 23, no. 4 (1999): 673-680.

[7] Gupta, R., K. T. Lai, M. Missous, and S. K. Haywood. "Subband nonparabolicity estimated from multiple intersubband absorption in highly doped multiple quantum wells." *Physical Review B* 69, no. 3 (2004): 033303.

[8] Broekaert, Tom PE, and Clifton G. Fonstad. "Novel, Organic Acid-Based Etchants for InGaAlAs/InP Heterostructure Devices with AlAs Etch-Stop Layers." *Journal of The Electrochemical Society* 139, no. 8 (1992): 2306-2309.

[9] Ling, H. S., S. Y. Wang, C. P. Lee, and M. C. Lo. "High quantum efficiency dots-in-a-well quantum dot infrared photodetectors with AlGaAs confinement enhancing layer." *Applied Physics Letters* 92, no. 19 (2008): 193506.

[10] El Mashade, Mohamed B., M. Ashry, and A. Nasr. "Theoretical analysis of quantum dot infrared photodetectors." *Semiconductor science and technology* 18, no. 9 (2003): 891.

[11] G. Osbourn, "Strained-layer superlattices from lattice mismatched materials," *Journal of Applied Physics,* vol. 53, pp. 1586-1589, 1982.

[12] G. C. Osbourn, "Journal of Applied Physics," *Strained layer superlattices from lattice mismatch materials,* vol. 53, pp. 1586-1589, 1982.
[13] Vurgaftman, I., J. áR Meyer, and L. áR Ram-Mohan. "Band parameters for III–V compound semiconductors and their alloys." *Journal of applied physics* 89, no. 11 (2001): 5815-5875.
[14] Pryor, C. E., and M-E. Pistol. "Band-edge diagrams for strained III–V semiconductor quantum wells, wires, and dots." *Physical Review B* 72, no. 20 (2005): 205311..
[15] Micallef, J., and B. L. Weiss. "The refractive index of III–V semiconductor strained-layer superlattices." *Optical and quantum electronics* 23, no. 6 (1991): 669-684.
[16] Wu, D. H., Y. Y. Zhang, and M. Razeghi. "Room temperature operation of InxGa1− xSb/InAs type-II quantum well infrared photodetectors grown by MOCVD." *Applied Physics Letters*112, no. 11 (2018): 111103.
[17] Chen, Wei, Zhuo Deng, Daqian Guo, Yaojiang Chen, Yuriy Mazur, Yurii Maidaniuk, Mourad Benamara et al. "Demonstration of InAs/InGaAs/GaAs Quantum Dots-in-a-Well Mid-Wave Infrared Photodetectors Grown on Silicon Substrate." *Journal of Lightwave Technology* (2018).
[18] Kim, HoSung, Seung-Yeop Ahn, SangHyeon Kim, GeunHwan Ryu, Ji Hoon Kyhm, Kyung Woon Lee, Jung Ho Park, and Won Jun Choi. "InAs/GaAs quantum dot infrared photodetector on a Si substrate by means of metal wafer bonding and epitaxial lift-off." *Optics express* 25, no. 15 (2017): 17562-17570.
[19] Palmer, D. W. "Growth and Characterisation of Semiconductors." *RA Stradling and PC Klipstein, Eds* (1990): 187.
[20] T. H. Gfroerer, "Photoluminescence in Analysis of Surfaces and Interfaces." *Encyclopedia of Analytical Chemistry,* (2000) pp. 9209-9231.
[21] Wolde, Seyoum, Yan-Feng Lao, A. G. Unil Perera, Y. H. Zhang, T. M. Wang, J. O. Kim, Ted Schuler-Sandy, Zhao-Bing Tian, and S. Krishna. "Noise, gain, and capture probability of p-type InAs-GaAs quantum-dot and quantum dot-in-well infrared photodetectors." *Journal of Applied Physics* 121, no. 24 (2017): 244501.